The Institute of Space and Astronautical Science
Report SP No. 17 March 2003

Influences of Transport Model on Heating Rate of Reentry Vehicles

By

Hirotaka OTSU*, Kazuhisa FUJITA† and Takashi ABE†

(1 February 2003)

Abstract: We assessed the effect of the models of transport properties for the estimation of the hypersonic reentry heating environment from an engineering point of view. Among the transport properties, we focus on the diffusion of chemical species. For this purpose, the following three models; Stefan-Maxwell model, Yos model, and Lee model are evaluated. The nominal flight condition for the evaluation is the reentry speed of 11.6 km/s at the altitude of 64 km, which corresponds to the most severe reentry flight condition for a super-orbital reentry such MUSES-C mission. In the nominal flight condition case, under both the non-catalytic wall condition and the full-catalytic wall condition, the Lee model shows a discrepancy with the other two models and gives a higher heat flux. On the contrary, the Stefan-Maxwell model and the Yos model show a reasonably good agreement between them. The discrepancy between the Lee model and the others is caused by the contribution of diffusion of enthalpy. The discrepancy between the Lee model and the others increases with an increase of the flight velocity while the discrepancy shows only a negligible dependency on the atmospheric density. The increase of the discrepancy is attributed to the increase of the chemical species of dissociated air with the increase of the flight velocity. Because of this, even the Lee model is acceptable in a low reentry speed range such a reentry from LEO. However the Lee model is hardly acceptable for an application to the higher velocity reentry such as a super-orbital reentry. On the other hand, the discrepancy between the Stefan-Maxwell model and the Yos model is reasonably small in all the circumstance. As for the calculation cost, the Stefan-Maxwell model is about two times expensive than other two models. Therefore, in a view point of estimating the heat flux for the hypersonic reentry flight vehicle with a reasonably accuracy and a reasonably computation cost, the Yos model is the most recommendable among the three models considered in this study.

1. Introduction

One of the key technologies for reentry missions is the development of the thermal protection system (TPS) for the reentry vehicle. For the design of TPS, the estimation of the heat flux to the reentry vehicle is a most critical subject. Among the heat flux to the reentry vehicle, which comprises of the convective and radiative parts, we will focus on the convective heat flux

* Shizuoka University, Johoku 3-5-1, Hamamatsu, Shizuoka 432–8561, JAPAN.
† The Institute of Space and Astronautical Science, Yoshinodai 3-1-1, Sagamihara, Kanagawa 229–8510, JAPAN.

in this study. This is because the radiative heat flux is smaller than the convective heat flux even in a hyperbolic reentry which is required for MUSES-C mission (Kawaguchi et al. 1996) and, therefore, the convective heat flux was of primary interest for the reentry vehicle.

For the estimation of the convective heat flux in the real flight condition, the ground experimental facility can not attain the real flight condition. Hence the computational fluid dynamics (CFD) technique is an alternative and promising method for the estimation of the convective heat flux. Needless to say, in order to obtain a reliable result from the CFD calculation, a suitable selection of the flow model, such as chemical reactions, thermal non-equilibrium and transport phenomena, is very important for an accurate estimation of the aerodynamic heating. This is because the flow model has a strong influence on the prediction of the flow field.

In the MUSES-C mission, the flow around the capsule is predicted to be thermally and chemically nonequilibrium at the altitude where the aerodynamic heating reaches its maximum value. In such a flow, the convective heat flux is composed of three terms; the conduction of energy due to the gradient of translational-rotational temperature, T, the conduction of energy due to the gradient of vibrational-electronic temperature, T_V, and the diffusion of enthalpy due to the concentration gradients of each chemical species. In the boundary layer, both temperatures are expected to be almost in equilibrium. Thus, the thermal conductivity inherent to them reflects an amount of the heat flux arising from their gradient at the boundary. The third term is related to the diffusion. All the three components are expected to be strongly dependent on the transport properties such the heat conductivity and the diffusion coefficients. This means that the models for the transport properties must be accurate and the accuracy of the models for the transport coefficients will have a large impact on the estimation of the convective heat flux to the reentry vehicle. Hence we must pay much attention to the selection of the models of transport properties for estimation of the convective heat flux. Among the transport properties, the model for the heat conductivity widely-accepted (Gnoffo et al. 1989) is comparably reliable while there are several models for the diffusion coefficients. In this study, we evaluate numerically the widely-used models for the diffusion coefficient in a view point of both the accuracy in an estimation of the reentry heating environment under the various reentry flight conditions and the computational cost.

2. Aerothermal models

In this study, we consider an aerodynamic heating environment for the super-orbital reentry such as the MUSES-C mission (Kawaguchi et al. 1996; Otsu et al. 1998). To assess numerically the aerodynamic heating environment, the following governing equation for the thermally and chemically nonequilibrium flow (Gnoffo et al. 1989) is employed;

$$\frac{\partial U}{\partial t} + \frac{\partial F_j}{\partial \xi_j} = S, \tag{1}$$

where U, F_j, and S are the vector of conserved quantities, flux vector, and the source vector, respectively. Park's two-temperature model (Park 1987) for thermal nonequilibrium is taken into account. In this model, the translational and rotational temperatures are regarded as a common temperature T, while the vibrational temperature of each molecule, electronic excitation temperature of each species, and translational temperature of free electron are regarded as another common temperature T_V. The vector of conserved quantities U is as follows;

$$U = (\rho_s, \rho u_j, \rho e, \rho e_V)^t, \tag{2}$$

where ρ_s is the density of each species, u_j is a flow velocity, e is the total energy of per unit mass, and e_V is the summation of the vibrational energy of each molecule, the translational energy of free electron, and the electronic excitation energy per unit mass. The vibrational energy of each species is calculated based on the harmonic oscillator model, while the first two terms of the partition function are taken into account for the electronic excitation energy of each species.

The relaxation time for the translational-vibrational energy exchange is calculated using the semi-empirical correlation proposed by Millikan and White (Millikan & White 1963) with the correction term suggested by Park (Park 1987). As for the molecular energy transfer process in which a certain amount of energy is removed at dissociation or is added at recombination of molecules, the amount of the energy is set to be 30% of the dissociation energy of each molecules (Sharma et al. 1988), which is called "preferential dissociation model" (Park 1990).

For chemical reactions, we considered 11 species for air consisting of N, O, N_2 , O_2, NO, N^+, O^+, $N_2{}^+$, $O_2{}^+$, NO^+, and e^-. As for the rate coefficients for the chemical reactions in a high temperature air, the Park's reaction set (Park 1990) for air species is considered.

2.1 Diffusion models

The existing diffusion models give a value of diffusion coefficient which slightly differs from each other while the difference may have a large impact on the distribution of chemical species near the wall and, therefore, on the convective heat flux. In this study, we took account of the three models which are currently widely-used. The brief descriptions of each model are given in the following section. The thermal conductivities and viscosity are calculated by the method written in the reference (Gnoffo et al. 1989) with tabulated data of the reference (Gupta et al. 1990).

Stefan-Maxwell model

The Stefan-Maxwell model is believed to be the most sophisticated model for the multi-species diffusion coefficients. In the model, the mole fraction gradient is represented by means of the diffusion flux and the diffusion coefficient in a following way;

$$\nabla x_i = \frac{M}{\rho} \sum_{j \neq i} \left(\frac{x_i J_j}{M_j \mathcal{D}_{ij}} - \frac{x_j J_i}{M_i \mathcal{D}_{ij}} \right), \tag{3}$$

where J_i and $\mathcal{D}_{ij}$ are the diffusion flux of species i and the binary diffusion coefficient for a pair of species i, j respectively.

Here we introduce the effective diffusion coefficient D_{im} for species i is defined in the following form,

$$\frac{(1 - x_i)}{D_{im}} = \sum_{j \neq i} \frac{x_j}{\mathcal{D}_{ij}}. \tag{4}$$

Then eq. (3) can be rewritten to solve for the diffusion flux of species i in the following form;

$$J_i = -\rho \frac{M_i}{M} \frac{D_{im}}{(1 - x_i)} \nabla x_i + \frac{c_i}{(1 - x_i)} D_{im} \sum_{j \neq i} \frac{M J_j}{M_j \mathcal{D}_{ij}}. \tag{5}$$

Since either equation (3) or (5) is a set of $(n-1)$ equations for n species, a closure equation is required to solve them. The closure equation is given by the mass conservation equation;

$$\sum_i J_i = 0 \tag{6}$$

A set of equations based on eq. (3) and eq. (6) must be solved simultaneously. In this study, this set of equations is solved by an iterative method. To accomplish this, we employ the following equation instead of the closure equation eq. (6);

$$J_i^{N+1} = J_i^N - c_i \sum_j J_j^N \tag{7}$$

where the superscript N means the number of iteration. In this iterative method, we solve the following equation for eq. (5);

$$J_i^{N+1} = -\rho \frac{M_i}{M} \frac{D_{im}}{(1-x_i)} \nabla x_i + \frac{c_i}{(1-x_i)} D_{im} \sum_{j \neq i} \frac{M J_j^N}{M_j \mathcal{D}_{ij}}, \tag{8}$$

being combined with eq. (7). After sufficient converge is attained starting from an initial guess for J_i^0, the solution satisfies a set of equations; i.e., eq. (5) and eq. (6). This iteration was repeated for 10 times typically.

Yos model

Yos model is based on an analogy with the binary diffusion which is given in terms of mole fraction;

$$J_i = -\rho \frac{M_i}{M} \left(\frac{1-c_i}{1-x_i} \right) \mathcal{D}_{ij} \nabla x_i. \tag{9}$$

In the Yos model, the binary diffusion coefficient $\mathcal{D}_{ij}$ for a pair of species i, j is replaced by the effective diffusion coefficient, D_{im}. Thus, the diffusion mass flux for species i for the Yos model is written in the following form,

$$\begin{aligned} J_i &= -\rho \frac{M_i}{M} \left(\frac{1-c_i}{1-x_i} \right) D_{im} \nabla x_i \\ &= -\rho \frac{M_i}{M} \left(\frac{1-c_i}{\sum_{j \neq i} (x_i / \mathcal{D}_{ij})} \right) \nabla x_i. \end{aligned} \tag{10}$$

where D_{im} is calculated using eq. (4).

To see a relation between the Yos model and the Stefan-Maxwell model, eq. (5) can be rearranged in the following form,

$$J_i = -\rho \frac{M_i}{M} \left(\frac{1-c_i}{1-x_i} \right) D_{im} \nabla x_i + \frac{c_i}{1-x_i} D_{im} \sum_{j \neq i} \left(\rho \frac{M_i}{M} \nabla x_j + \frac{M}{M_j} \frac{J_j}{\mathcal{D}_{ij}} \right). \tag{11}$$

As it shows, the difference between the Yos model and the Stefan-Maxwell model arises from the second term of eq. (11). (Sutton & Gnoffo 1998)

Lee model

In the Lee model, the binary diffusion coefficient in eq. (10) is approximated by using the common diffusion coefficient D, (Cander & MacCormack 1988)

$$\frac{1-x_i}{D} = \sum_{j \neq i} \frac{x_j}{\mathcal{D}_{ij}} \tag{12}$$

where D is calculated by the following relation,

$$D = \frac{\mu}{\rho S_c}. \tag{13}$$

In this study, the Schmidt number, S_c, is assumed to be constant and is set to be 0.5.

Using this common diffusion coefficient D and eq. (10), the diffusion flux of species i for the Lee model is defined as follows,

$$J_i = -\rho \frac{M_i}{M} \left(\frac{1-c_i}{1-x_i} \right) D \nabla x_i. \tag{14}$$

Comparison of eq. (10) with eq. (14) tells that the Lee model is an approximation of the Yos model, in that D_{im} in the Yos model is replaced by a common value of D.

3. Numerical methods

To solve eq. (1), we employed the Advection Upstream Splitting Method (AUSM) type scheme (Liou & Steffen 1993; Wada & Liou 1994). This type of scheme can capture a stationary discontinuity with negligible numerical dissipation and is robust enough to calculate the shock waves and expansion waves. Additionally, this scheme is of a flux splitting type, which is suitable to its application to a large system of equations. As for the stiffness problem related to the strong dissociation and ionization reactions, a diagonal implicit method (Otsu et al. 1998; Bussing & Murman 1985; Eberhardt & Imlay 1990) was employed. The total number of the computational grid was 1800 points, 30 points along the body surface and 60 points along the line normal to the body surface.

3.1 Calculation cost

All the calculations were performed on the computer with a CPU chip of Alpha 21264/600 MHz and 256 MB RAM. A steady solution is obtained after a sufficient iteration based on the time-marching method.

To compare the performance of the various models, the accuracy of the calculated result is of a primary importance. However the computational cost to accomplish it is also important. To measure the computational cost, the CPU time necessary to carry out 1000 iterations was compared for the three models. Each CPU time was shown on Table 1. From this table, the CPU time of the Stefan-Maxwell model is found to be about 2 times larger than that of the Lee model, while the Yos model requires almost the same cost with the Lee model.

4. Results and Discussions

As for a nominal situation for the flow field calculation, we consider the flight condition of MUSES-C mission. In the flight condition, we focus on the flight condition at which the

reentry capsule encounters the peak convective heat flux; i.e., the reentry flight velocity of 11.6 km/s at the altitude of 64 km. The MUSES-C reentry capsule has a configuration of a sphere cone with a 45-deg. half angle, a nose radius of 20 cm, a sharpened shoulder, and a flat base. The boundary condition at the vehicle surface is imposed in a way that the wall temperature is fixed at 3000 K. At the vehicle surface, we investigate both the non-catalytic wall condition and the full-catalytic wall condition to examine their influence on the effect the diffusion models. Under the non-catalytic wall condition, the concentrations of neutral species are calculated by assuming a vanishing diffusive flux except ions and electron. As for the ions and electron, their concentration at the surface is set to be zero. This is because the electronic neutrality at the surface of the vehicle must be attained. This means that the surface is treated as a catalytic one for the ions and electron even under the non-catalytic wall condition. On the other hand, under the full-catalytic wall condition, the concentrations of all the species are set to become the same value as the free stream condition.

4.1 Flow characteristics on the stagnation line

In this section, a brief description of flow characteristics at the stagnation region is given. Here we focus on the nominal flight condition; i.e., the reentry flight velocity of 11.6 km/s at the altitude of 64 km. As for the boundary condition at the surface, the non-catalytic wall condition is imposed. The temperature distribution along the stagnation line is shown in Fig 1. The translational-rotational temperature, T, reaches the maximum value at X = 14 mm, while the vibrational-electronic temperature, T_V, is still much lower than T. T_V begins to be equilibrated around at X = 6 mm and continues to be equilibrated until the surface. On the contrary, the thermal nonequilibrium is observed at the region adjacent to the equilibrium region; i.e., from X = 16 mm to X = 6 mm. The equilibrated temperature amounts up to about 12000 K.

Figure 2 shows the distribution of chemical species. From these figures, we can see that N_2 and O_2 molecules dissociate rapidly and, successively, the generation of NO molecule, the atomic nitrogen and oxygen, and the ionization of the molecules such as N_2, O_2 and NO, occur rapidly in the thermal nonequilibrium region. Then, after the rapid generation, the molecular species rapidly begins to dissociate. In the thermal equilibrium region, the ionic atoms N^+ and O^+ are created. The mass fraction of atomic ions such as N^+ and O^+ amount up to around 0.14 and 0.03 respectively. These values are relatively high compared to the one expected for the low reentry speed condition. Besides the atomic ions, the dissociation proceeds more extensively in this speed range than in the low reentry speed range.

Effect of diffusion models on the flow properties near the surface

Now, we will see the effect of the each diffusion models on the flow characteristics. The results shown in this section are for the nominal reentry flight condition with non-catalytic wall condition. Figure 3 shows the temperature distributions near the surface. In the region far from the surface, the temperature for the Lee model is slightly (about 500 K) lower than

Table 1: CPU time of 1000 iterations for the three models.

Model	Lee	Stefan-Maxwell	Yos
CPU time [s.]	663.20	1393.82	660.94

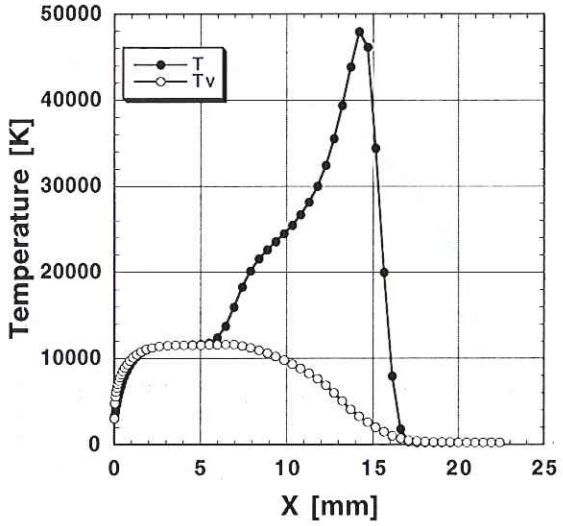

Fig. 1: Temperatures distribution on the stagnation line under the nominal flight condition.

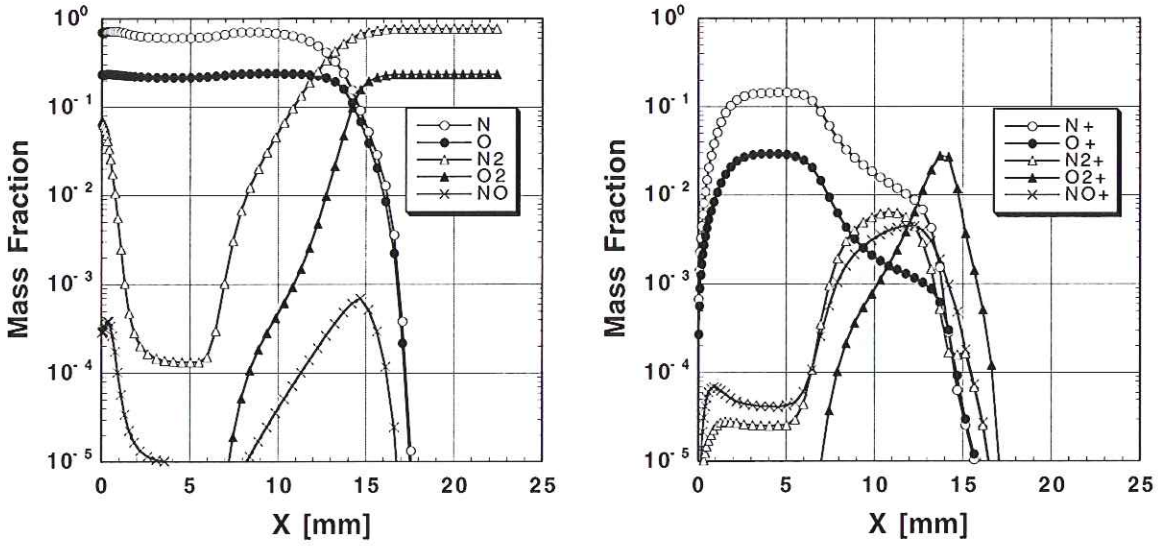

Fig. 2: Distribution of mass fraction of chemical species on the stagnation line under the nominal flight condition.

that of other two diffusion models while, in the region close to the surface, the difference among the diffusion models is negligibly small. This suggests that the heat flux derived from the temperature gradient is almost independent on the diffusion model. In contrast to the temperature distribution, the behavior of the mass fraction of chemical species depends on the diffusion model as shown in Fig. 4 where the distribution of mass fraction of N^+ is depicted for the three diffusion models. The distribution of N^+ near the surface for the Lee model clearly differs from that of other two models, and is steeper than that in the other models. This suggests that the heat flux derived from the diffusion of ionic species may depends on the model. We will argue about this subject in the following sections.

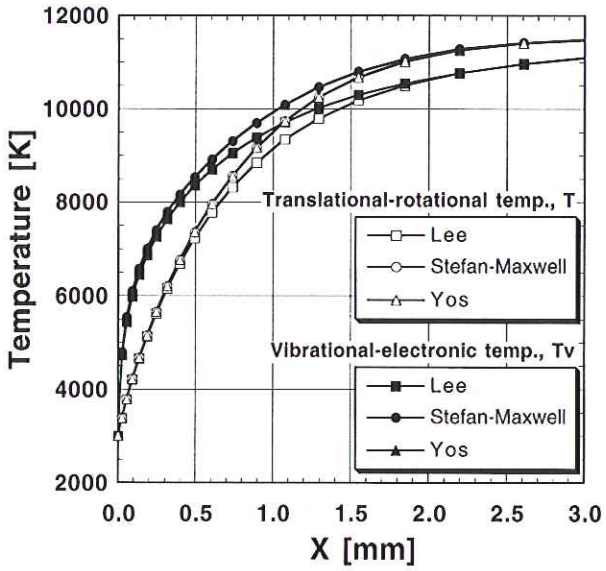

Fig. 3: Temperatures distribution on the stagnation line for the three models.

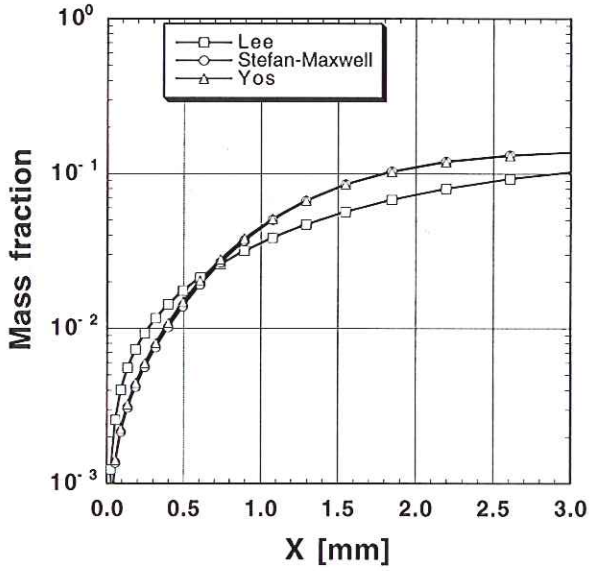

Fig. 4: Distribution of mass fraction of N^+ on the stagnation line for the three models.

4.2 Heat flux estimation at the stagnation

The aerodynamic heat flux is a sum of the contribution from the translational and vibrational temperature gradients, the diffusion of enthalpy of ions/electrons, and the other neutral species. The influence of the diffusion model appears differently in each contribution and also is affected by various conditions such as the wall catalysity and flight conditions. In the following sections, we will investigate the influence of the diffusion model on the heat flux under various conditions.

Effect of wall catalysity

Under the non-catalytic wall condition, the main source of the convective heat flux is the conduction of energy due to the gradients of T and T_V as shown in Fig. 5, even though a contribution from the diffusion of enthalpy (that is, the diffusion of ions/electrons) still exists. In both the Stefan-Maxwell model and the Yos model, the contribution from the diffusion of enthalpy is negligibly small and almost the same amount of heat flux is predicted since their temperature profiles near the surface are almost identical as discussed above. In the Lee model, however, the contribution of the diffusion is not small and the heat flux higher than the other models is predicted since the contribution of the temperature gradients is almost the same as that in the other models. That is, the difference between them arises from the heat flux related to diffusion of ions/electrons.

Under the full-catalytic wall condition, as can be seen in Fig. 6, the heat flux contributed from the diffusion of the chemical species, especially the diffusion of neutral species, becomes significant. This is because, near the surface, the concentration of neutral species is much larger than that of ions, and the temperature distribution is almost unaffected by the wall catalysity. On the contrary, the contribution from the temperature gradient is almost the same as the one predicted in the non-catalytic wall condition. Because of this, the heat flux under the full-catalytic wall condition is much larger than that under the non-catalytic wall condition. In the Lee model, the contribution from the diffusion is larger than that in the other models even though the ions/electron contribution becomes small being compared to that under the non-catalytic wall condition. Hence, the Stefan-Maxwell model and the Yos model gives a similar value for the heat flux, while the one for the Lee model is larger than the others.

Effect of the reentry flight velocity

Besides the wall catalysity, it is expected that the variation of flight condition may affect the appearance of the model dependency since the variation of the flight condition gives rise to the variation of flow characteristics which may affect the aerodynamic heat flux. In this section, we investigate the behavior how the appearance of the model dependency depends on the flight condition. As for the reentry flight condition, the reentry flight velocity and the atmospheric density are considered.

To examine the effect of flight velocity, the reentry flight velocity is varied from 9.0 km/s to 13.0 km/s including the nominal value inbetween, while the density is fixed as a nominal value.

From Fig. 7, it is observed that the larger the reentry flight velocity is, the larger the convective heat flux is. This is the case in all the diffusion models. Though the result by the Stefan-Maxwell model and the Yos model shows a similar trend with the increasing velocity, the result by Lee model differs from the others. The discrepancy between them becomes larger with the larger flight velocity. This behavior is observed not only in the case of the non-catalytic boundary condition but also in the case of the catalytic boundary condition. As discussed above, the discrepancy between the Lee model and the other models is derived from the contribution of the diffusion of enthalpy of the chemical species. Hence this increase in the discrepancy is because the number of chemical species of dissociated air becomes significant with the increasing flight velocity, since the larger the flight velocity is, the stronger the shock wave is and, behind the stronger shock wave, the chemical reactions proceeds more extensively.

As mentioned above, we can see that the difference between the Yos model and the Stefan-Maxwell model is very small. This means that the Yos model can predict the convective heat

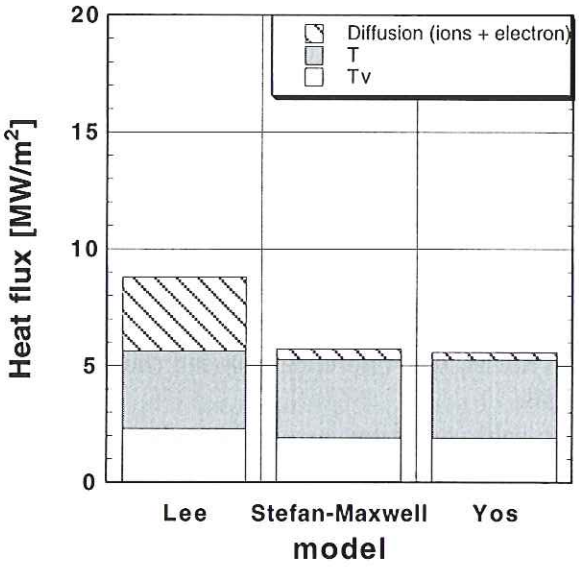

Fig. 5: Comparison of convective heat flux under the non-catalytic wall condition.

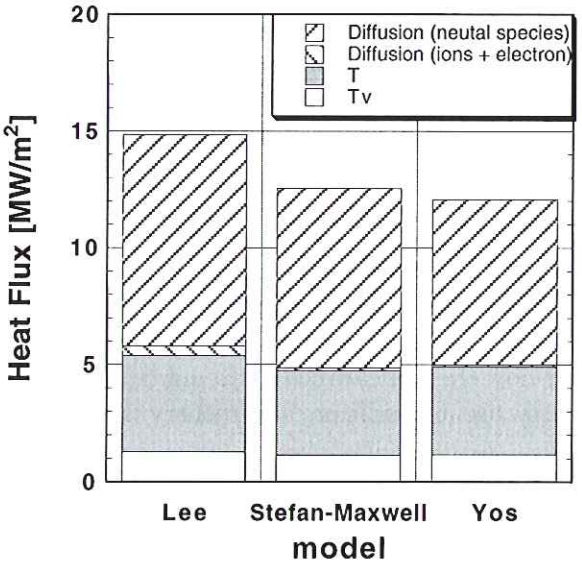

Fig. 6: Comparison of convective heat flux under the full-catalytic wall condition.

flux with almost the same accuracy of the Stefan-Maxwell model under the flight velocity range between 9.0 km/s and 13.0 km/s. Also it should be mentioned that, in a low speed range such as 9 km/s, the discrepancy between the Lee model and the other models is reasonably small while the discrepancy can not be neglected in the reentry speed range inherent to the super-orbital reentry. That is, in a low speed range, the Lee model can be acceptable while, in the higher reentry speed, the Lee model is hardly acceptable.

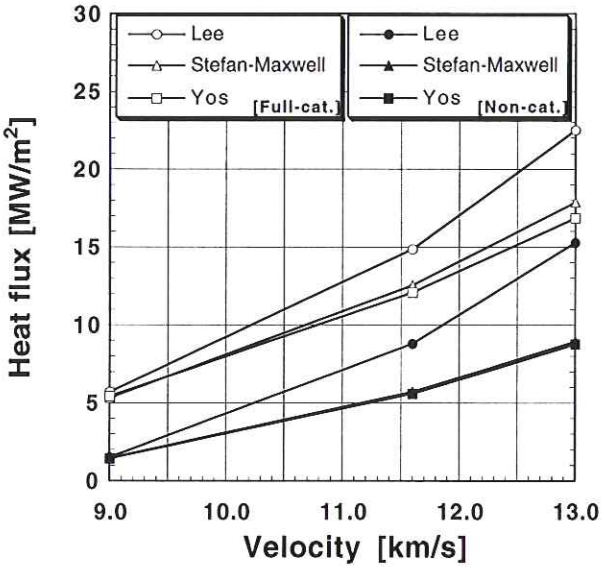

Fig. 7: Effect of the reentry flight velocity and diffusion models on the total convective heat flux.

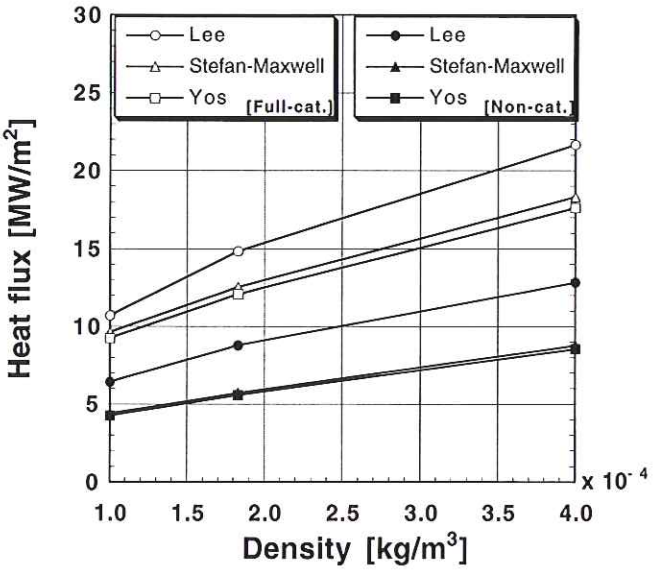

Fig. 8: Effect of the total density and diffusion models on the total convective heat flux.

Effect of the atmospheric density

In this section, we will examine the effect of the atmospheric density on the heat flux. To this aim, the atmospheric density was varied from 1.0×10^{-4} kg/m^3 to 4.0×10^{-4} kg/m^3 including the nominal value inbetween, while the reentry flight velocity is fixed as the nominal value. The variation of the atmospheric density corresponds to the variation of the flight altitude.

The heat flux at the stagnation increases with the increasing atmospheric density as shown in Fig. 8. Though the result by the Stefan-Maxwell model and the Yos model reasonably agrees to each other, the result by the Lee model differs from the others. The discrepancy between

them, however, shows only a slight dependency on the increase of the density. This is the case not only in the case of the catalytic wall condition but also in the case of the non-catalytic wall condition.

5. Conclusion

In this study, we assessed the models for diffusion coefficients in a view point of the application to simulate the hypersonic reentry heating environment. The nominal flight condition for the assessment is the reentry speed of 11.6 km/s at the altitude of 64 km which corresponds to the flight condition for the peak aerodynamic heating during the super-orbital reentry. Three diffusion models; the Stefan-Maxwell model, the Yos model, and the Lee model, are evaluated. The Stefan-Maxwell model is the most sophisticated while the Yos model is an approximation of the Stefan-Maxwell model. The Lee model is a further approximation of the Yos model, and is the simplest among them.

In the nominal flight condition case, under both the non-catalytic wall condition and the full-catalytic wall condition, the Lee model shows a discrepancy with the other two models and gives a higher heat flux. On the contrary, the Stefan-Maxwell model and the Yos model show a reasonably good agreement between them. The discrepancy between the Lee model and the others is derived from the extent of the contribution of diffusion of enthalpy of the chemical species.

In order to investigate the effect of the reentry flight condition on the heat flux, the effect of the reentry flight velocity and the atmospheric density was investigated. The discrepancy between the Stefan-Maxwell model and the Yos model is reasonably small in all the circumstance. On the other hand, there is a discrepancy between the Lee model and the others. The discrepancy between the Lee model and the others increases with an increase of the velocity while the discrepancy shows only a negligible dependency on the atmospheric density. This increase of the discrepancy is attributed to the increase of the chemical species of dissociated air with the increase of the velocity. Because of this, even the Lee model is acceptable in a low reentry speed range such a reentry from LEO. However the Lee model is hardly acceptable for an application to the higher velocity reentry such as a super-orbital reentry.

As for the calculation cost, the Stefan-Maxwell model is about two times more expensive than the other two models.

From these results, we can conclude that, in a view point of estimating the heat flux for the super-orbital reentry flight vehicle with a reasonably accuracy and a reasonably computation cost, the Yos model is the most recommendable among the three models considered in this study.

According to the present investigation, the diffusion model has a significant influence on the accuracy of the prediction for the heat flux. This, in return, suggests that we should pay more attention to the selection of the models for other transport properties and the further investigations in modeling the transport phenomenon are important for the accurate estimation of the heat flux.

REFERENCES

Kawaguchi, J., Fujiwara, A., and Sawai, S., "Sample and Return Mission from Asteroid Nereus via Solar Electric Propulsion," *Acta Astronautica*, Vol. 38, No. 2, 1996, pp. 87-101.

Otsu, H., Suzuki, K., Fujita, K., and Abe, T., "Radiative Heating Analysis around the MUSES-C Reentry Capsule at a Superorbital Speed ," AIAA Paper, AIAA 98-2447, June, 1998.

Park, C., "Assessment of Two-Temperature Kinetic Model for Dissociating and Weakly Ionizing Nitrogen," AIAA Paper, AIAA 86-1347, June, 1987.

Gupta, R. N., Yos, J. M., Thompson, R. A., and Lee, Kam-Pui, "A Review of Reaction Rates and Thermodynamic and Transport Properties for an 11-Species Air Model for Chemical and Thermal Nonequilibrium Calculations to 30,000 K," NASA RP-1232, 1990.

Park, C., *Nonequilibrium Hypersonic Aerothermodynamics,* John Wiley & Sons, Inc., 1990.

Gnoffo, P. A., Gupta, R. N., and Shinn, J. L., "Conservation Equations and Physical Models for Hypersonic Air Flows in Thermal and Chemical Nonequilibrium," NASA TP-2867, 1989.

Candler, G. V. and MacCormack, R. W., "The Computation of Hypersonic Ionized Flows in Chemical and Thermal Nonequilibrium," AIAA Paper, AIAA 88-0511, January, 1988.

Millikan, R. C., and White, D. R., "Systematics of Vibrational Relaxation," *Journal of Chem. Phys.,* Vol. 39, No. 12, Dec. 1963, pp. 3209-3213.

Park, C., "Assessment of Two-Temperature Kinetic Model for Ionizing Air," AIAA Paper, AIAA 87-1574, June, 1987.

Sutton, K., and Gnoffo, P. A., "Multi-Component Diffusion with Application To Computational Aerothermodynamics," AIAA Paper, AIAA 98-2575, 1998.

Liou, M.-S. and Steffen, C. J., "A New Flux Splitting Scheme," *Journal of Computational Physics,* Vol. 107, No. 1, 1993, pp. 23-39

Wada, Y. and Liou, M.-S. "A Flux Splitting Scheme with High-Resolution and Robustness for Discontinuities," AIAA Paper, AIAA 94-0083, January, 1994.

Bussing, T. R. A. and Murman, E. M., "A Finite Volume Method for the Calculation of Compressible Chemically Reacting Flows," AIAA Paper, AIAA 85-0331, 1985.

Eberhardt, S. and Imlay, S. "A Diagonal Implicit Scheme for Computing Flows with Finite-Rate Chemistry" AIAA Paper, AIAA 90-1577, June, 1990.

Sharma, S. P., Huo, W., and Park, C., "The Rate Parameters for Coupled Vibration-Dissociation in Generalized SSH Theory," AIAA Paper, AIAA 88-2714, 1988.